Fluorescence Lifetime Imaging Ophthalmoscopy (FLIO) in Eyes With Pigment Epithelial Detachments Due to Age-Related Macular Degeneration

Lydia Sauer, Christopher B. Komanski, Alexandra S. Vitale, Eric D. Hansen, and Paul S. Bernstein

Department of Ophthalmology and Visual Sciences, John A. Moran Eye Center, University of Utah, Salt Lake City, Utah, United States

Correspondence: Paul S. Bernstein, John A. Moran Eye Center, University of Utah, 65 Mario Capecchi Drive, Salt Lake City, UT 84132, USA; paul.bernstein@hsc.utah.edu.

Submitted: February 11, 2019
Accepted: June 10, 2019

Citation: Sauer L, Komanski CB, Vitale AS, Hansen ED, Bernstein PS. Fluorescence lifetime imaging ophthalmoscopy (FLIO) in eyes with pigment epithelial detachments due to age-related macular degeneration. *Invest Ophthalmol Vis Sci*. 2019;60:3054–3063. https://doi.org/10.1167/iovs.19-26835

Purpose. To investigate fluorescence lifetime imaging ophthalmoscopy (FLIO) in neovascular AMD and pigment epithelial detachments (PEDs).

Methods. A total of 46 eyes with PEDs (>350 µm) as well as age-matched healthy controls were included in this study. We found 28 eyes showed neovascular AMD (nvAMD), and 17 had nonneovascular (dry) AMD (dAMD). The Heidelberg Engineering FLIO excited fluorescence at 473 nm. Fluorescence decays were detected in two spectral channels (498–560 nm; 560–720 nm) to determine fluorescence lifetimes of endogenous fluorophores in their specific spectral emission ranges. Mean fluorescence lifetimes (τ_m) were investigated. Multimodal imaging was reviewed by two ophthalmologists who circumscribed and classified PEDs as either serous ($n = 4$), hemorrhagic ($n = 4$), fibrovascular ($n = 16$), drusenoid ($n = 17$), or mixed ($n = 5$). Blood samples from a healthy subject and a patient with PED were investigated in a quartz cuvette.

Results. Eyes with nvAMD show similar FLIO patterns to dAMD: ring-shaped prolongations of τ_m 3 to 6 mm from the fovea. Different PED-forms show characteristic τ_m, while serous and hemorrhagic PEDs exhibit shortened τ_m, drusenoid PEDs show prolonged τ_m, and τ_m in fibrovascular PEDs is variable. Areas corresponding to sub-/intraretinal fluid display shortened τ_m. Ex vivo studies of blood also show short τ_m.

Conclusions. The previously described dAMD-related FLIO pattern is also present in nvAMD. Short τ_m in serous, fibrovascular, and hemorrhagic PEDs as well as sub/intraretinal fluid may disrupt this pattern. FLIO appears to differentiate between PEDs, hemorrhage, and fluid. Additionally, ex vivo studies of human blood help to better interpret FLIO images.

Keywords: FLIO, fluorescence lifetime imaging, age-related macular degeneration, lipofuscin, blood

Age-related macular degeneration (AMD), a major vision threatening disease for individuals above 65 years, can either remain as nonneovascular or lead to the formation of choroidal and/or retinal neovascularization. Neovascularization can be treated with injections of antivascular endothelial growth factor antibodies and antibody fragments.[1–3] However, due to the development of macular atrophy, not all eyes with neovascular AMD (nvAMD) will maintain good visual acuity.[4] Overall, therapeutic outcomes in both nvAMD and nonneovascular (dry) AMD (dAMD) are not satisfying.[2–6] More research needs to be done to find out about metabolic circumstances and changes in the diseased retina. The environment as well as individual genetic risk factors are involved in AMD pathogenesis.[7–10] Extracellular debris deposits called drusen are currently recognized as the hallmark pathologic feature of AMD.[10,11] Complement dysregulation and chronic inflammation seem to play a key role in drusen as well as in AMD development.[12–14] However, the full metabolic pathways still remain unknown. The formation and fate of pigment epithelial detachments (PEDs) in AMD are of special interest, as they often represent an initial step of vision loss.[15] PEDs can have different histologic subtypes, which can be classified as drusenoid, fibrovascular, serous, and hemorrhagic.[15]

The novel retinal imaging modality known as fluorescence lifetime imaging ophthalmoscopy (FLIO) may detect metabolic and disease-related changes within the retina.[16–18] Healthy eyes without AMD risk factors show a characteristic FLIO lifetime pattern with shortest FLIO lifetimes in the fovea and longest at the optic disc.[19–21] Drusen in donor tissue were also previously investigated with time-resolved FAF imaging.[22] AMD seems to present specific lifetime patterns in FLIO, and recently, it has been shown that eyes with dAMD exhibit a very specific pattern of prolonged FLIO lifetimes.[23] A different FLIO study on AMD also found a general prolongation of FLIO lifetimes in AMD.[24]

Fluorescence lifetime imaging in general is a sensitive method to detect changes within the microenvironment of cells.[25] It has been shown that even changes in the oxidative state of cells or the pH may show altered fluorescence lifetimes.[26] Imaging fluorescence lifetimes in the retina likely shows minor changes in the retina as well.[17,18] However, as the retina is more complex than individual tissue sections, the assignment of altered fluorescence lifetimes to specific fluorophores is more difficult. As FLIO is a very novel technique, its exact sensitivity has not yet been investigated, and longitudinal studies will be necessary to truly evaluate the sensitivity of this novel methodology. Previously, using the

experimental FLIO device, Schweitzer et al.[27] determined the sensitivity and specificity for discrimination of healthy subjects and diabetic patients who have no sign of diabetic retinopathy. In this study, the SSC showed a sensitivity of 83.8% and a specificity of 84% for τ_2, and in the LSC, the best separation was found within τ_3 (sensitivity: 89.2 %; specificity 80%).[27]

Nevertheless, as specific patterns of FLIO lifetimes can be assigned to specific retinal diseases, early changes of retinal lifetime patterns are likely disease-related. The described AMD FLIO pattern appears in some healthy age-matched subjects as well, which may be a sign of risk to develop AMD in the future.[23] Many other diseases have been investigated with FLIO, where this novel technique was reported to be beneficial.[28–40] This study focuses on describing FLIO lifetimes in patients with PEDs due to dAMD as well as nvAMD.

Methods

This cross-sectional study was conducted at the John A. Moran Eye Center in Salt Lake City, UT, USA. The University of Utah Institutional Review Board (IRB) approved this study, which adhered to the tenets of the Declaration of Helsinki. Prior to any investigations, informed written consent was obtained from all patients. All measurements were performed between March 2017 and December 2018. One patient was imaged and included at a later time point in May 2019. This 69-year-old male initially presented with a fibrovascular PED in May 2019 and received FLIO imaging before his first intravitreal anti-VEGF injection that same day. He subsequently presented 2 weeks later with a new hemorrhagic PED. Due to the uniqueness of this case, we decided to include this patient to our study.

Procedure

Patients as well as control subjects were examined and diagnosed by an ophthalmologist prior to inclusion. Each patient and healthy subject underwent a FLIO measurement with dilated pupils. The patients received multimodal imaging, always including OCT scans (Spectralis; Heidelberg Engineering, Heidelberg, Germany). Intraocular pressure was assessed with a Tonopen, with all study procedures completed prior to performance of any fluorescein angiography procedures. Multimodal imaging including OCT, fundus photography, FAF intensity imaging and in some cases including fluorescein angiography, was reviewed by two ophthalmologists blinded to FLIO results. These two ophthalmologists identified PEDs >350 µm, circumscribed the location of the PED based on multimodal imaging, and classified the PED as either drusenoid, serous, fibrovascular, hemorrhagic, or mixed based on the classification by Pepple and Mruthyunjaya.[15] In three eyes from three different patients, the graders results did not match. In these cases, the grading of the senior specialist was used. However, in all of these cases, the final diagnosis was mixed serous and fibrovascular PED, whereas one grader had graded the PED as only one part of it (either serous or fibrovascular). The graders also determined whether the patient had dAMD or nvAMD; there was no difference in the grading. dAMD includes only eyes that never before showed neovascularization. The graders also determined the presence of sub- or intraretinal fluid; there was no difference in the grading. Subsequently, fluorescent lifetimes were obtained for each circumscribed area using individual masks based on the circumscribed localization of PEDs.

FLIO

The FLIO device setup, safety and image acquisition have previously been described in detail elsewhere.[16,20,21,34] Relying on the principle of time-correlated single photon counting, the prototype FLIO is based on an imaging platform (Heidelberg Engineering) and is suited to record FLIO lifetimes in vivo.[16,41] FAF intensity and lifetime images were acquired from a 30° field centered at the fovea (excitation wavelength 473 nm). Photons were detected in two separate spectral channels: a short spectral channel (SSC; 498–560 nm) and a long spectral channel (LSC; 560–720 nm). A high-contrast confocal infrared reflectance (IR) image for eye tracking was included.

Fluorescence data were analyzed using imaging software (SPCImage 4.4.2; Becker & Hickl GmbH, Berlin, Germany). The fluorescence decay was approximated by calculating the least-square fit of a series of three exponential functions; 3×3-pixel binning was applied. The amplitude weighted mean fluorescence decay time (τ_m) was used for further analysis. Additional details have been described elsewhere.[21,41]

To obtain FLIO lifetimes from the areas of PEDs, masks for the areas of PEDs were manually created by one of the graders. The grader used multimodal imaging to determine the area of PED, blinded to FLIO. After this, the grader drew the previously outlined area onto the FAF intensity image in the imaging software (Becker & Hickl GmbH). The software automatically overlays this mask onto the FLIO image and provides mean FLIO lifetimes for both spectral channels from the area of the mask. To obtain FLIO lifetimes from the AMD pattern, the outer ring (OR) from a standardized Early Treatment of Diabetic Retinopathy Study (ETDRS) grid was analyzed. However, to exclude PED fluorescence from within this area, manual masks were drawn to exclude the areas of PEDs. The same grader drew all of the masks.

SPC-Image and FLIMX were used for all FLIO lifetime analysis and to illustrate the FLIO lifetimes.[42] The FLIMX software is documented and freely available for download online under the open source BSD-license (http://www.flimx.de).

Ex Vivo Measurement of Blood

Blood anticoagulated with ethylenediaminetetraacetate was obtained from a healthy 40-year-old volunteer, as well as one patient that presented with a new-onset hemorrhagic PED. Fluorescence lifetimes of blood were measured in a quartz cuvette over 2 hours, while the blood was left to separate into plasma and sedimented erythrocytes. Throughout the course of 2 hours the autofluorescence lifetimes were recorded intermittently. After 2 hours, the blood sample was shaken to combine both layers, and autofluorescence lifetimes were measured again.

Data analysis was performed using SPC-Image. As fluorescence lifetimes were similar between a bi- and tri-exponential fitting approach, the samples were fitted using a tri-exponential fit and a binning of 1 to keep it uniform with the patient analysis. Details about fitting process of ex vivo samples have been described elsewhere.[43] Mean fluorescence lifetimes in the region of the cuvette were averaged over a square of 100×100 pixels.

Statistical Analysis

A standardized ETDRS grid was used to obtain τ_m from different regions of interest, and statistical software (SPSS 21; SPSS Inc., Chicago, IL, USA) was employed in all statistical analyses. To test for significant τ_m differences between different eyes, an independent sample *t*-test was used. Our data followed normal distribution (checked with the Kolmogorov-Smirnov test), and all results are provided as mean ± standard deviation (SD). A Bonferroni correction was applied in case of multiple testing. Although one patient was imaged at two time points and showed different forms of PED at each point (fibrovascular, hemorrhagic), this patient was only included once in the statistical analysis (as a hemorrhagic PED).

Investigative Ophthalmology & Visual Science

Table 1. Characterization of Investigated Subjects

Demographics	Healthy	PED
Eyes, *n*	45	46
Subjects, *n*	26	35
Mean age ± SD, y	66 ± 9	76 ± 8
IOL, *n* (%)	14 (31)	19 (41)
Sex, *n* (%)	F: 13 (50) M: 13 (50)	F: 17 (49) M: 18 (51)

Results

Subjects

This study includes a total of 46 eyes from 35 patients with PED due to AMD. The mean age was 76 ± 8 years (range 60–90 years). We found 29 of these eyes showed nvAMD, and 17 had dAMD. Additionally, an age-matched group of 45 eyes from 26 healthy subjects (mean age: 66 ± 9 years) was included. A detailed characterization of all subjects is given in Table 1.

All investigated PEDs were larger than 350 µm. PEDs were classified according to Pepple and Mruthyunjaya[15] as either serous ($n = 4$ eyes), hemorrhagic ($n = 4$ eyes), fibrovascular ($n = 16$ eyes), drusenoid ($n = 17$ eyes), or mixed ($n = 5$ eyes). Of the 5 eyes with mixed PEDs, one was a hemorrhagic plus fibrovascular PED, while all others were serous plus fibrovascular PEDs. All 17 drusenoid PEDs were from eyes with dAMD, and all other PEDs were from eyes with nvAMD.

Two special cases were additionally included in the study but not in any statistical analysis. The first case was an eye with an RPE tear. This female patient was 84 years old at examination date and showed nvAMD with a fibrovascular PED in her other eye. The second case was a 74-year-old female with subretinal hyperreflective material (SHRM). Due to retinal fibrosis, this eye was not included in any further statistical analysis.

Typical FLIO Pattern in Eyes With nvAMD

A typical and consistent FLIO pattern can be observed in all eyes with AMD, regardless of whether the eye shows neovascular or nonneovascular AMD. In eyes with AMD, FLIO lifetimes are prolonged in a ring-shaped area between the large arcade vessels in an area between 3 and 6 mm from the fovea. The pattern is most prominent in the LSC. Figure 1 shows this pattern in one eye with dAMD and one eye with nvAMD, as well as one healthy eye. The OR describes the area of prolonged FLIO lifetimes in AMD. The OR showed significantly prolonged FLIO lifetimes in eyes with nvAMD (SSC: 369 ± 62 ps; LSC: 470 ± 36 picoseconds [ps]), as well as dAMD (SSC: 388 ± 78 ps; LSC: 438 ± 32 ps), compared to age-matched healthy eyes (SSC: 327 ± 80 ps; LSC: 361 ± 63 ps). The complete statistical analysis can be found in Table 2.

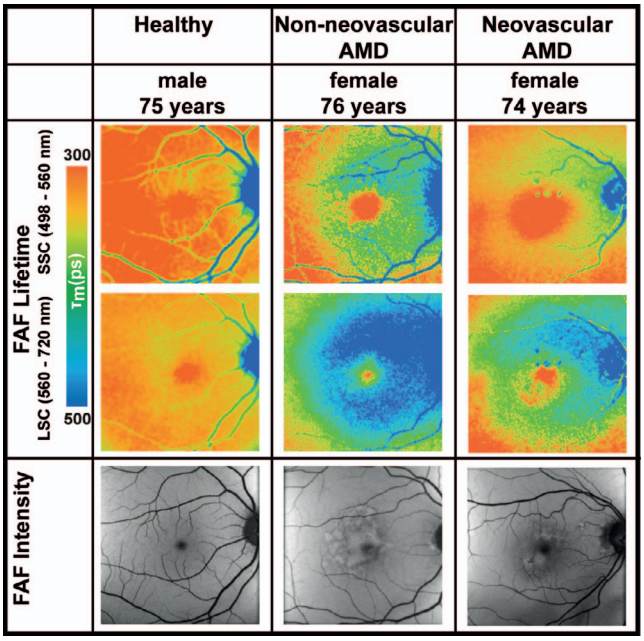

Figure 1. FLIO lifetime images from the both spectral channels (SSC: 498–560 nm and LSC: 560–720 nm) as well as FAF intensity image of one healthy eye, one eye with nonneovascular age-related macular degeneration, and one eye with neovascular AMD. Healthy: fovea SSC, 160 ps; LSC, 305 ps; outer ring SSC, 258 ps; LSC, 347 ps. Nonneovascular AMD: fovea SSC, 211 ps; LSC, 356 ps; outer ring SSC, 397 ps; LSC, 465 ps. Neovascular AMD: fovea SSC, 128 ps; LSC, 232 ps; outer ring SSC, 319 ps; LSC, 410 ps.

FLIO Lifetimes in Areas of PED

FLIO lifetimes in areas of pigment epithelial detachment showed both prolonged as well as shortened FLIO lifetimes.

Table 2. Mean FLIO Lifetimes in Healthy Subjects and AMD Patients

Area of Interest	Healthy ($n = 45$)	Neovascular AMD ($n = 29$)	Non-neovascular AMD ($n = 17$)	*P* Value: Healthy and Neovascular AMD	*P* Value: Healthy and Nonneovascular AMD	*P* Value: Neovascular and Nonneovascular AMD
Central area (C)						
SSC, ps	223 ± 80	152 ± 63	190 ± 76	**<0.001**	0.135	0.066
LSC, ps	309 ± 66	273 ± 79	296 ± 58	0.062	0.464	0.303
Outer ring (OR)						
SSC, ps	327 ± 80 ps	369 ± 62	388 ± 78	**<0.05**	**<0.01**	0.353
LSC, ps	361 ± 63 ps	470 ± 36	438 ± 32	**<0.001**	**<0.001**	**<0.05**
Difference (OR minus C)						
SSC, ps	104 ± 26	217 ± 56	198 ± 40	**<0.001**	**<0.001**	0.219
LSC, ps	53 ± 26	196 ± 75	141 ± 57	**<0.001**	**<0.001**	**<0.05**
Area of PED						
SSC, ps	NA	302 ± 91	349 ± 59	NA	NA	0.058
LSC, ps	NA	409 ± 72	435 ± 102	NA	NA	0.682

Bolded *P* values indicate statistical significance.

Table 3. Mean FLIO Lifetimes in Different PEDs

PED Type	SSC, ps	LSC, ps
Drusenoid ($n = 17$)	349 ± 59	435 ± 102
Fibrovascular ($n = 16$)	309 ± 103	419 ± 84
Serous ($n = 4$)	297 ± 23	396 ± 31
Hemorrhagic ($n = 4$)	289 ± 69	298 ± 46

All drusenoid PEDs are from eyes with nonneovascular AMD, whereas all other PED types are from eyes with neovascular AMD.

This likely originates from different pathomechanisms behind the PED. Table 3 shows mean FLIO lifetimes from different forms of PED. Drusenoid PEDs show longest FLIO lifetimes in either spectral channel, serous PEDs show shortest FLIO lifetimes in the SSC, and hemorrhagic PEDs show shortest lifetimes in the LSC. Fibrovascular PEDs may show either short or long FLIO lifetimes; this may be due to the different constitutions of fluid and fluorescent material. Figure 2 depicts one eye of each PED type (drusenoid, fibrovascular, serous, and hemorrhagic). Figure 3 gives some additional examples of patients with PEDs.

A 69-year-old male presented initially with a fibrovascular PED and received FLIO imaging but was initially not included in this study (past recruitment time). He received his first anti-VEGF injection at this timepoint and presented 2 weeks later with a hemorrhagic PED. Figure 4 shows his FLIO images before and after he developed a hemorrhagic PED, as well as his blood sample measurements. The patient had a natural lens.

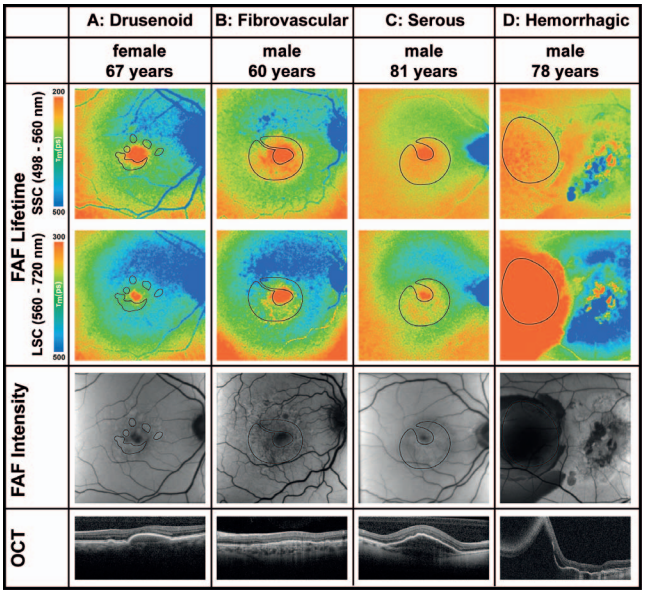

Figure 2. FLIO lifetime images from the both spectral channels (SSC: 498–560 nm and LSC: 560–720 nm) as well as FAF intensity and OCT images of four eyes from patients with different types of pigment epithelial detachments associated with age-related macular degeneration. Masks highlight the area of PEDs. FLIO data: (**A**) Fovea SSC, 188 ps; LSC, 297 ps; outer ring SSC, 414 ps; LSC, 447 ps; areas of PED SSC, 354 ps; LSC, 419 ps. (**B**) Fovea SSC: 84 ps; LSC: 189 ps; outer ring SSC, 378 ps; LSC, 513 ps; areas of PED SSC, 249 ps; LSC, 403 ps. (**C**) Fovea SSC, 165 ps; LSC, 320 ps; outer ring SSC, 322 ps; LSC, 424 ps; areas of PED SSC, 266 ps; LSC, 317 ps. (**D**) Fovea SSC: 253 ps; LSC, 384 ps; outer ring SSC, 313 ps; LSC, 486 ps; areas of PED SSC, 240 ps; LSC, 250 ps.

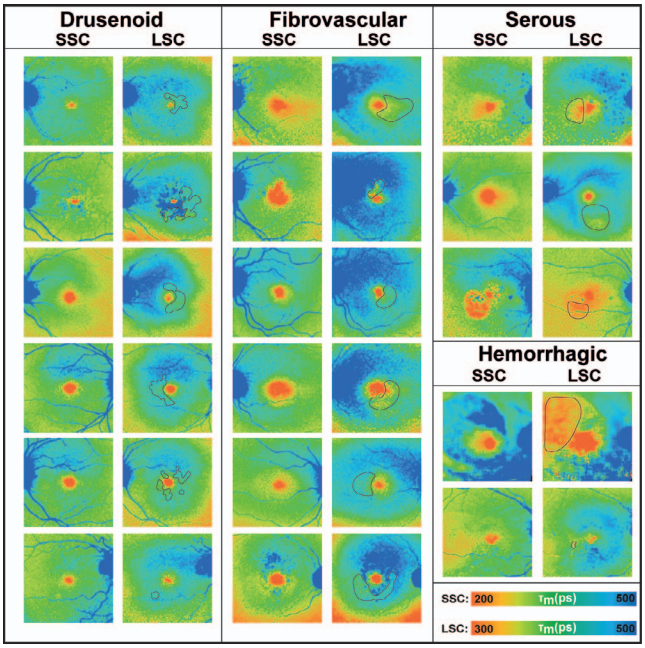

Figure 3. FLIO lifetime images from the both spectral channels (SSC: 498–560 nm and LSC: 560–720 nm) of eyes with different types of PED.

FLIO Lifetimes in One Patient With an RPE Tear

FLIO lifetimes were investigated in one case of an RPE tear. The patient was an 84-year-old female with a fibrovascular PED in her second eye. The patient had an artificial IOL. The eye with the RPE tear is shown in Figure 5. Due to the tear, an area of blood can be found adjacent to areas of RPE atrophy. In FLIO imaging, areas of blood have considerably shorter FLIO lifetimes (SSC: 128 ps; LSC: 226 ps; red color) compared to healthy areas of the fundus (SSC: 253 ps; LSC: 384 ps). Areas of RPE atrophy show much prolonged FLIO lifetimes (SSC: 427 ps; LSC: 475 ps; blue color).

FLIO Lifetimes in One Patient With Subretinal Hyperreflective Material

SHRM was observed in one eye that also showed retinal fibrosis in other areas. The area with SHRM exhibited shortened FLIO lifetimes, Figure 6 shows the images of this eye. In this 74-year-old female, who had an artificial IOL, the AMD-related area (OR) showed FLIO lifetimes of 296 ps (SSC) and 433 ps (LSC). SHRM showed similar lifetimes in the SSC (284 ps), but much shorter mean FLIO lifetimes in the LSC (316 ps). FLIO lifetimes of adjacent fibrotic areas were much prolonged (SSC: 455 ps; LSC: 640 ps).

FLIO Lifetimes in Retinal Vessels

In most eyes, the retinal vessels show long decay times. However, short lifetimes were also occasionally observed at some blood vessels. Fourteen of the 46 investigated eyes showed some vessels with short FLIO lifetimes. In one patient, both eyes showed short vessel lifetimes. In two other patients, the second eye did not show short vessel lifetimes. For all other patients, the second eye was not included in this study. These vessels with short FLIO lifetimes were always veins and tended to show a large vessel diameter. All but one eye showed neovascular AMD. All but two eyes had artificial intraocular lenses. The two eyes with the short vessel lifetimes and natural lens are both eyes of the same patient; this patient showed

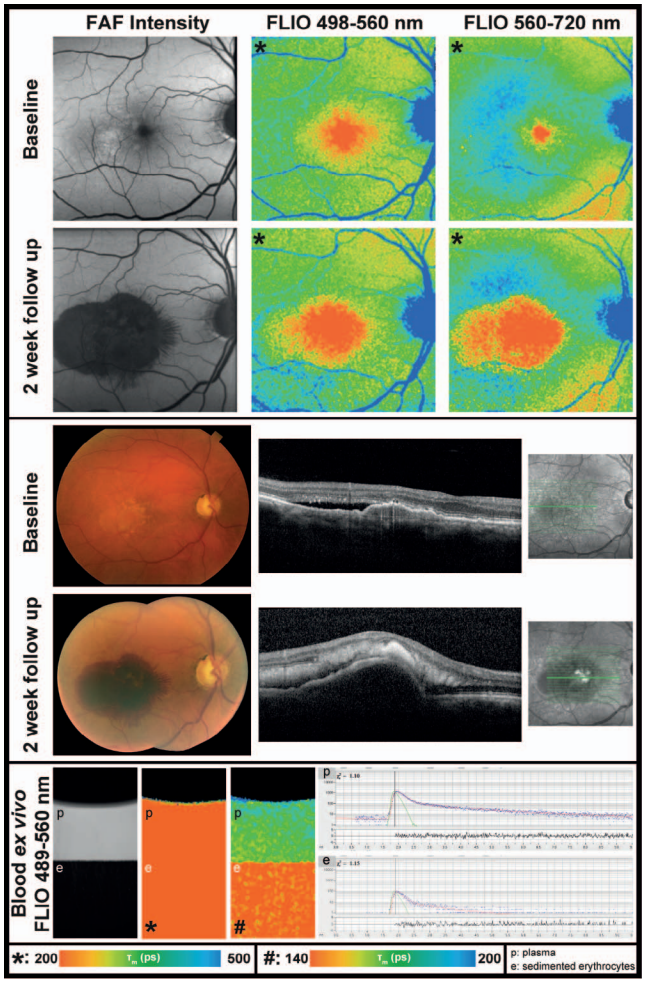

Figure 4. FAF lifetime and intensity images from the both spectral channels (SSC: 498–560 nm and LSC: 560–720 nm) as well as OCT image and color fundus photograph of one eye before and after development of a hemorrhagic PED. The patient has a natural lens. In addition, ex vivo measurements of blood from this patient in a cuvette (at time point 120 minutes) are presented. Further blood data can be found in Table 4.

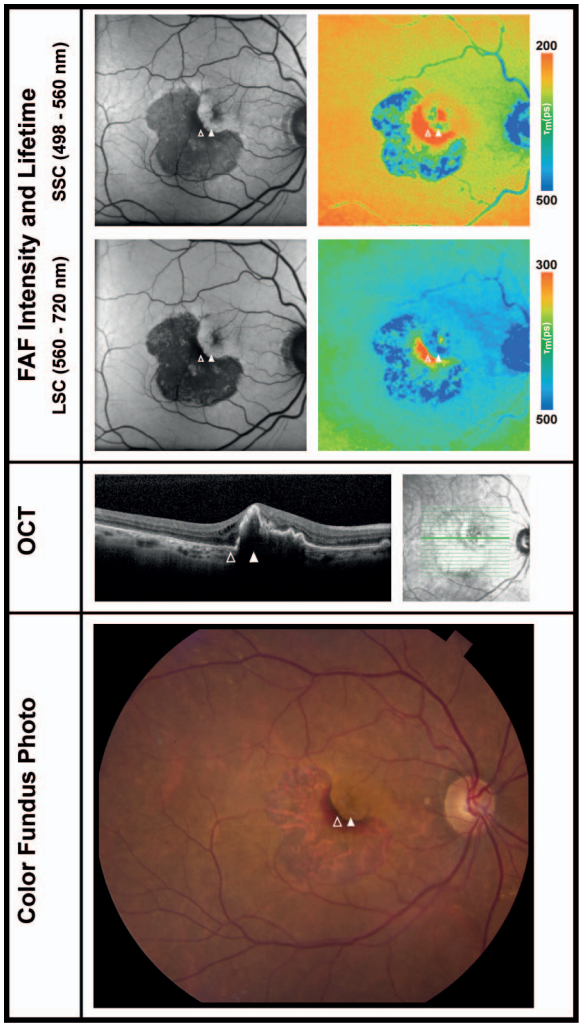

Figure 5. FAF intensity and lifetime images from the both spectral channels (SSC: 498–560 nm and LSC: 560–720 nm) as well as OCT image and color fundus photograph of one eye with an RPE tear. The *outlined arrows* point to an area of intraretinal blood, the *full arrows* point to the area of RPE. The patient has an artificial intraocular lens. FLIO data: areas of blood SSC: 128 ps, LSC: 226 ps; unaffected areas of the fundus SSC: 253 ps, LSC: 384 ps; areas of RPE atrophy SSC: 427 ps, LSC: 475 ps.

clear natural lenses without any signs of cataract. Six eyes with short vessel lifetimes were from male patients, and eight were from female patients. The mean age of patients that showed short vessel lifetimes was 78 ± 11 years. This observation was made not only in patients with AMD, but also other diseases as well as healthy eyes. One patient with AMD and short FLIO lifetimes within the vessels is presented in Figure 7.

Ex Vivo Fluorescence Characteristics of Blood

Blood showed relatively short mean autofluorescence lifetimes. Initially after the blood was drawn, autofluorescence lifetimes around 165 ps (SSC) and 220 ps (LSC) were found. The autofluorescence lifetimes shortened over that time period in the settled erythrocytes. Conversely, we observed slightly longer lifetimes in the plasma portion. When the blood sample was shaken after 2 hours, the autofluorescence lifetimes became comparable to the initial measurement. The corresponding data are presented in Table 4. The first subject from which the blood was drawn had a healthy FLIO pattern and long lifetimes at the vessels, and the second subject's images are shown in Figure 4 before and after his hemorrhagic PED.

The Influence of the Lens

We found that 27 of the investigated eyes had a natural lens, and 19 of the investigated eyes had an IOL. Cataract was an exclusion criterion, but due to the advanced age, patients with natural lenses showed traces of nuclear sclerosis. Table 5 shows the analysis of patients and healthy subjects with different lenses.

Investigating the fovea as well as the OR separately, significant differences can be found only within the SSC. By investigating differences between these two regions, there is no significant difference between patients with natural lenses or intraocular lenses.

Investigating PEDs, these lifetimes were significantly shorter for patients with an IOL. However, the distribution of PED types was not uniform between these groups. In the group with natural lenses were 14 drusenoid, 7 fibrovascular, 2 serous, 2 hemorrhagic, and 2 mixed PEDs. The group with IOL showed three drusenoid, nine fibrovascular, two serous, two hemorrhagic, and three mixed PEDs. The drusenoid PEDs

Investigative Ophthalmology & Visual Science

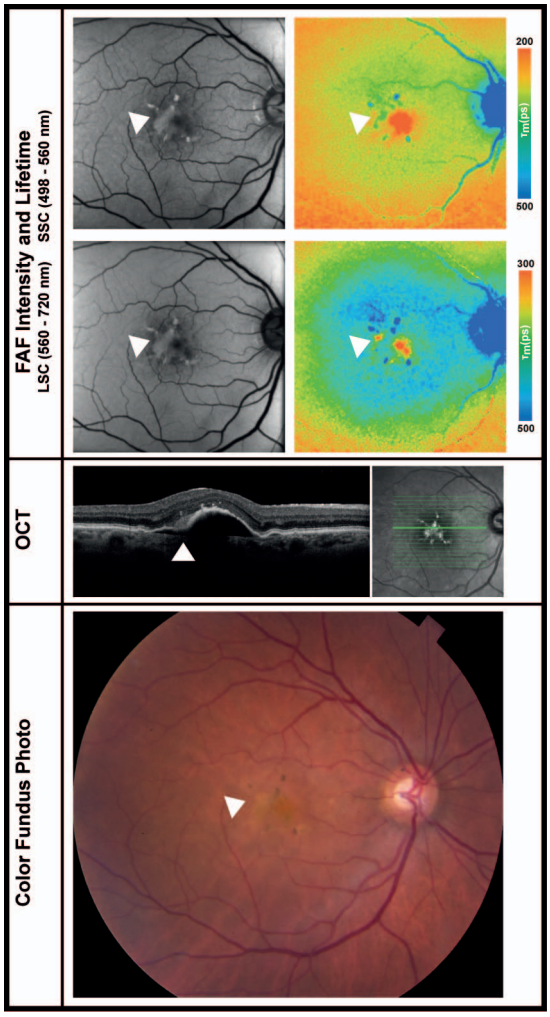

Figure 6. FAF intensity and lifetime images from the both spectral channels (SSC: 498–560 nm and LSC: 560–720 nm) as well as OCT image and color fundus photograph of one eye with SHRM. The *arrows* point at the area of SHRM. The patient had an artificial IOL. FLIO data: areas of SHRM SSC: 284 ps, LSC: 316; fibrotic areas SSC: 455 ps, LSC: 640 ps; fovea SSC: 114 ps, LSC: 300 ps; outer ring SSC: 296 ps, LSC: 433 ps.

especially, which show longest FLIO lifetimes, are not distributed homogeneously. The area of the OR does not show significant differences in the LSC between patients with natural lenses and IOL, and the spectrum of fluorescence intensity from the lens is located predominantly in SSC and only minimal in LSC. We therefore believe that these differences may actually be due to the different types of PEDs included in the subgroups.

Discussion

Metabolic changes in AMD may occur even before they are detectable with conventional imaging techniques.[44] FLIO imaging seems to be helpful in detecting such changes at early stages.[23] The technique of in vivo retinal autofluorescence lifetime imaging was first introduced by Schweitzer et al.[45] Many FLIO studies have focused on improving the method and continuing the investigation of specific disease-related FLIO lifetime patterns.[16–18,20,21,33,37,39] Healthy eyes exhibit a well described and reproducible pattern.[20,21] Short FLIO lifetimes

Table 4. Mean FLIO Lifetimes of Blood

	Subject 1, Male, 40 y, Healthy				Subject 2, Male, 69 y, AMD			
Time, min	SSC, ps	LSC, ps	SSC, ps	LSC, ps	SSC, ps	LSC, ps	SSC, ps	LSC, ps
0	165*	220*	–	–	160*	218*	–	–
30	160*	210*	–	–	155*	210*	–	–
60	150†	205†	183‡	255‡	143†	199†	168‡	242‡
120	150†	200†	176‡	285‡	144†	194†	175‡	244‡
125§	164*	220*	–	–	159*	219*	–	–

Subject 2 is presented in Figure 7.
* Whole blood.
† Sedimented erythrocytes.
‡ Plasma.
§ Blood sample was shaken at this time.

are localized in the fovea and caused by the autofluorescence of retinal carotenoids, whereas long lifetime fluorescence is localized at the area of the optic nerve, presumably caused by connective tissue. Intermediate-long FLIO lifetimes can be found across the retina as they are thought to indicate the impact of lipofuscin. This pattern seems to be different for AMD eyes where FLIO lifetimes are prolonged.[23,24,31,40,46] The prolongation of mean FLIO lifetimes is strongest in the LSC and may be caused by an early accumulation of bis-retinoids in the RPE.[24,33,44] Early FLIO lifetime imaging studies have shown that the autofluorescence in the LSC is predominantly influenced by lipofuscin.[17] The intermediate-long τ_m were also associated with lipofuscin.[34] This pattern spans a broad area 3-6 mm from the foveal center between the large vessel arcades, corresponding to the area of the OR and is most pronounced in the superior and nasal area and least pronounced temporally. However, the intensity of the pattern can vary and may correlate with disease progression. This specific FLIO pattern was previously described for eyes with dAMD.[23] Eyes with nvAMD also show this typical AMD-related pattern. This may indicate that similar processes can occur in both forms, and the blunt division between nvAMD and dAMD may not be correct, as both forms feature similar FLIO characteristics. Although FLIO lifetimes in the fovea are shorter for patients with AMD compared to healthy subjects, likely due to the high rate of patients on carotenoid supplements (39 out of 46 eyes are from patients on long-term supplements), the FLIO lifetimes of the OR are significantly prolonged for both forms of AMD. However, it should be noted that there is a difference in the pattern presentation between nvAMD and dAMD. In certain areas of neovascularization, short FLIO lifetimes are observed. This disrupts the typical FLIO pattern in some eyes with nvAMD, alluding to different mechanisms of this disease. An example of this disruption of the typical FLIO pattern can be seen in Figure 2, where the area of the serous PED in the LSC shows short fluorescence lifetimes which disrupts the typical AMD pattern of ring-shaped prolonged FLIO lifetimes.

PEDs are a typical feature of AMD. These can be of different forms, with different properties and exhibiting distinct lifetimes. The knowledge of these properties may help the ophthalmologist to distinguish between different forms, which may require specific treatment. As FLIO is a noninvasive technology, this could potentially substitute for more invasive procedures such as fluorescein angiography. OCT-A appears to be very helpful in detecting neovascularization, but in combination with FLIO, this technique could be enhanced as not only structural but also metabolic information could be obtained from retinal tissue. FLIO therefore is an addition to

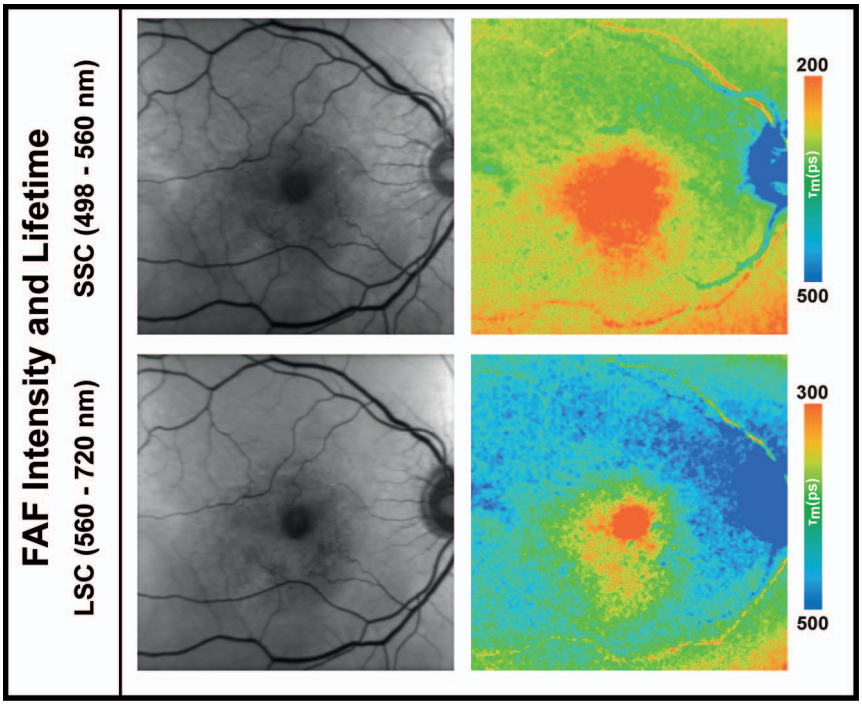

Figure 7. FAF intensity and lifetime images from the both spectral channels (SSC: 498–560 nm and LSC: 560–720 nm) from one eye with short FLIO lifetimes at the vessels. FLIO data: Fovea SSC, 102 ps; LSC, 295 ps; outer ring SSC: 307 ps; LSC, 496 ps; areas of PED SSC: 214 ps; LSC, 418 ps.

conventional retinal imaging and may refine diagnostic possibilities.

In the present study, PEDs were investigated with FLIO in detail. We found that different PEDs may show both shortened as well as prolonged FLIO lifetimes. Previous studies investigated drusen in AMD and often came to the conclusion that drusen showed prolonged FLIO lifetimes.[17,18,22,23,46,47] However, one previous study described short FLIO lifetimes in the context of retinal drusen.[24] In PEDs, the different lifetimes seem to be associated with different forms of PEDs.

Drusenoid PEDs exhibited mostly prolonged FLIO lifetimes, which may be due to an accumulation of lipofuscin components as well as other substances. Nevertheless, drusenoid PEDs still showed shorter FLIO lifetimes compared to the AMD-related ring-shaped pattern. While not all drusen fluoresce equally, the FLIO lifetimes can vary depending on the individual druse. One patient in our study showed a drusenoid PED with relatively short FLIO lifetimes, which is inconsistent with typical FLIO lifetime prolongation in drusen. This patient previously had nvAMD, and while the PED appeared phenotypically to be drusenoid, it may actually be a vascularized PED. The shortened FLIO lifetimes may indicate differences of drusenoid PEDs in different forms of AMD that could represent variable pathomechanisms of AMD. Whether or not this difference of drusen lifetimes delineates between nvAMD and dAMD or finds indications for other subgrouping strategies needs to be investigated further.

Both serous as well as hemorrhagic PEDs showed shortened FLIO lifetimes compared to the healthy fundus. It is likely that the amount of fluid plays a role for the individual FLIO lifetimes in PED. Although we only investigated four hemorrhagic and four serous PEDs, the hemorrhagic PEDs seemed to show even shorter lifetimes. Larger serous PEDs also seemed to have shorter lifetimes than smaller serous PEDs. However, a larger

Table 5. Mean FLIO Lifetimes With Differences in the Lens Status

	Eyes From Patients with AMD			Eyes From Healthy Controls		
Area of Interest	**Natural Lens (n = 27)**	**IOL (n = 19)**	***P* Value**	**Natural Lens (n = 31)**	**IOL (n = 14)**	***P* Value**
Fovea						
SSC, ps	194 ± 75	133 ± 44	**<0.01**	236 ± 80	164 ± 44	**<0.05**
LSC, ps	299 ± 75	261 ± 61	0.082	317 ± 69	269 ± 28	0.059
Outer Ring						
SSC, ps	405 ± 74	339 ± 37	**<0.01**	340 ± 82	268 ± 33	**<0.05**
LSC, ps	457 ± 40	455 ± 35	0.879	368 ± 67	333 ± 29	0.167
Outer Ring Minus Fovea						
SSC, ps	212 ± 52	205 ± 49	0.691	104 ± 25	104 ± 28	0.991
LSC, ps	158 ± 75	194 ± 65	0.106	50 ± 25	64 ± 25	0.175
PED						
SSC, ps	343 ± 85	270 ± 67	**<0.01**	NA	NA	NA
LSC, ps	424 ± 53	379 ± 62	**<0.05**	NA	NA	NA

Bolded *P* values indicate statistical significance.

number of PEDs will need to be investigated to truly confirm this finding. In addition, we present a case of a patient that initially showed a fibrovascular PED, received his first injection of anti-VEGF after his baseline FLIO image, and returned within 2 weeks showing a new hemorrhagic PED. We obtained his blood for ex vivo investigation. Both, the hemorrhagic PED as well as his blood show short FLIO lifetimes.

We also investigated a case of a RPE tear and realized that the short lifetimes here were also associated with the presence of blood. We therefore speculate that fluid, both serous as well as hemorrhagic, causes the short fluorescence decays. In addition, however, for a thorough discussion we have to mention other potential causes of short lifetimes in the macular area. Besides the macular pigment, the RPE showed shortest lifetimes in single layers of ex vivo porcine eyes.[48] Short lifetimes here may arise from missing contribution of the inner layers of the retina, especially if they may be thinned due to the PED.[49] Nevertheless, as Figure 5 shows, the area where inner retinal layers are thinned shows longer FLIO lifetimes. As a variety of fluorophores contributes to the FLIO signal in vivo, we can only speculate that blood may be a source of short FLIO lifetimes.

Retinal vessels usually show long fluorescence decay times. However, we noted that in some instances short autofluorescence lifetimes can be observed at the areas of the vessels. These short lifetimes seem to be independent of gender as well as to the presence of diseases, as we have occasionally observed these short lifetimes within healthy subjects or young patients with retinitis pigmentosa (Fig. 4H in previously published work[38] as well as unpublished data). A significant portion of the eyes investigated in this study (14 out of 46 eyes) showed short lifetime vessels. All of these vessels were veins that were large in diameter. Interestingly, all but one of these patients showed nvAMD. However, as we have observed the short lifetime vessels in other diseases, we do not believe that these short lifetimes are disease-related. Another feature of all eyes with short lifetime vessels was that all but two of them had an artificial intraocular lenses, and the two cases with natural lens showed very clear lenses. Despite the confocality of FLIO, we believe that we observe a superposition of the lens fluorescence. In areas with strong retinal fluorescence intensity, this effect is rather small. In areas with weak fluorescence intensity, such as the vessels, the fluorescence of the blood/veins may be overlaid by the long fluorescence from the lens. This would occur in eyes with natural lenses and especially cataracts. In young patients (e.g., retinitis pigmentosa) as well as patients with artificial IOLs, the fluorescence signal from the veins can be observed because the lens fluorescence is not strong. Nevertheless, as not all young patients and not all patients with IOLs show these short lifetimes, we cannot exclude that other factors could play a role. In future studies it would be interesting to compare lifetimes characteristics of blood from subjects with and without short lifetime vessels. Despite not being able to prove this hypothesis, we believe that it is a possibility that the short lifetimes observed in vessels may originate from blood. This is supported by studies of blood ex vivo.

A previous study already described autofluorescence lifetimes of blood, but conditions to measure autofluorescence lifetimes differ from this study.[50] We therefore conducted ex vivo measurements of blood with our system, which gives us additional information as close to our in vivo system as possible. We found that blood in a quartz cuvette showed distinct fluorescence properties, which were very similar between two different subjects. The fluorescence intensity of whole blood was weak with short fluorescence lifetimes (SSC around 160 ps; LSC around 220 ps). As the blood separates into erythrocytes and plasma, the erythrocyte sediment remains to show a weak fluorescence, but the fluorescence intensity of the plasma was strong. The erythrocytes show shorter lifetimes, and the plasma part exhibits slightly longer lifetimes. Table 4 shows the data in detail. Overall, both lifetimes are still relatively short. Remixing the blood after two hours restored the initial fluorescence decays. Combining the findings of short vessel lifetimes with the ex vivo measurements of blood, which shows short fluorescence lifetimes, we believe that the blood inside the vessel shows short lifetimes, and only the edge of the vessel (e.g., connective tissue or muscle fibers in arterial walls) shows longer lifetimes. As the fluorescence intensity from the vessels is very weak (weaker than the foveal center), we believe that the long lifetimes may also be a superposition with long fluorescence lifetimes of the lens.

This study has some limitations. A rigorous grading of PEDs resulted in small numbers of patients in the individual groups. The group of pure serous PEDs was exceptionally small, as most serous PEDs have fibrovascular components and were therefore graded as mixed PEDs. Additionally, we included only four pure hemorrhagic PEDs, and one PED that was hemorrhagic as well as fibrovascular. The latter one was again graded as mixed. A larger study should confirm the findings, especially in these two subgroups of PED. As the mean age of our patients is fairly advanced, effects due to cataract of the lens cannot be excluded. Also, clear natural lenses exhibit a fluorescence with a long decay time in the range of 3 to 4 ns, predominantly in the SSC. Therefore, the impact of the fluorescence of the lens on fundus measurements is not only related to cataract.[51] Recently, Dysli and colleagues[24] described a dependence of the FLIO lifetimes in eyes with AMD on the lens status. Other FLIO-based studies did not find significant differences between natural lens and IOL.[23,34,39] We found that 41% of our patients had an IOL, equally divided between dAMD and nvAMD. In our study, the AMD-related pattern was visible regardless of the lens status. In a sub-analysis, we compared the FLIO lifetimes from areas of interest between patients with IOL and natural lenses. Only the SSC showed significant differences for the foveal area as well as the OR. The LSC did not show significant differences in these areas. This study focuses on the LSC; therefore, we believe that the lens does not interfere to a relevant degree. However, comparing lifetimes of PEDs between patients with IOL and natural lenses did show significant differences. We did not record the type of IOL that individual patients had, and therefore cannot exclude that the type of IOL may influence FLIO lifetimes to a minor degree. Although we cannot completely rule out a small influence of the lens, the fact that the pattern of the OR did not show significant differences makes it more likely that these actually are differences within the different PEDs in these groups. Drusenoid PEDs, which showed the longest lifetimes of all PEDs, were mostly found in eyes with a natural lens. This could explain the significant difference in the PED despite no significant difference in the OR. Due to small sample sizes and no significant differences of the OR of the LSC, we did not perform a subanalysis of different PED types in IOL patients only. This should be done in a larger study in the future. Furthermore, we performed FLIO measurements on just two blood samples. A thorough analysis of additional blood samples would be interesting in future studies to investigate whether carotenoid supplementation status plays a role in autofluorescence lifetimes of the blood. Finally, it would be interesting to investigate relations between individual fluorescence components and different forms of PED. The tri-exponentional model function holds detailed information that were not further investigated in this study. A previous study, comparing the fluorescence lifetime in healthy subjects and patients suffering from early AMD, found an explicit prolongation of fluorescence lifetimes for the second lifetime component (tau 2) in the SSC.[46] This relation, as well as other possible relations of the different

Investigative Ophthalmology & Visual Science

components and amplitudes should be evaluated in further studies.

Conclusions

The use of FLIO in clinical applications has produced consistent patterns associated with a great variety of retinal diseases. Deviations from the healthy FLIO pattern can guide ophthalmologists to find the correct diagnosis at a much earlier stage and potentially intervene before irreversible damage occurs. Of particular interest is the pattern found in AMD, which consistently presents in every patient with the disease. Furthermore, long-term longitudinal studies may confirm that this pattern may manifest in patients prior to development of the disease.

In order to truly understand these disease-related changes, it is important to understand the origin of individual lifetimes or lifetime components. This often is a difficult challenge, as FLIO is a noninvasive imaging device. Therefore, it takes multiple pieces of information to understand certain signals. This is the first study suggesting that short FLIO lifetimes that do not originate from the macular pigment may have their origin in fluid within the retina. Short lifetimes have previously been described for areas of central serous retinopathy.[32] Here, we describe the presence of short fluorescence lifetimes in areas of PED, where especially hemorrhagic PEDs showed short lifetimes. SHRM also showed short FLIO lifetimes, and it was previously described that SHRM could be composed of scar tissue, fluid and possibly hemorrhage. As morphologic data about SHRM is limited, the short lifetimes in FLIO imaging may give additional hints towards its morphological constitution. Furthermore, we are able to show that vessels occasionally show short lifetimes. Retinal artery occlusion, on the other hand, was found to show significantly longer lifetimes of affected areas.[28,52] Finally, the analysis of blood samples ex vivo gives additional evidence that blood and blood plasma show short fluorescence lifetimes. This is consistent with the interpretation that blood could be a potential source of short FLIO lifetimes in vivo as well. However, more work remains to confirm this hypothesis.

In conclusion, this study shows that the AMD-related FLIO lifetime pattern that has previously been described can be found in eyes with both dAMD as well as nvAMD. However, due to the presence of short autofluorescence decays in areas of PED, the pattern might be disturbed in some eyes. Short FLIO lifetimes outside of areas with macular pigment may be associated with fluid in the retina, such as blood or serous fluid. Short lifetimes in vessels as well as ex vivo studies of human blood samples support this hypothesis. Understanding the source of short FLIO lifetimes may help to better interpret FLIO images in a variety of different diseases, including age-related macular degeneration. Overall, FLIO is a promising new tool that may give further insights into the pathology and pathophysiology of AMD.

Acknowledgments

The authors thank Heidelberg Engineering for providing the FLIO as well as for their technical assistance. The authors especially thank Yoshihiko Katayama, PhD, for his technical assistance and Matthias Klemm, PhD, for providing the FLIMX software. The authors also thank all coworkers from the John A. Moran Eye Center and the Sharon Eccles Steele Center for Translational Medicine who helped recruit and image the patients. The authors especially thank the clinical studies team of the Moran Eye Center.

Supported by the National Eye Institute of the National Institutes of Health under award numbers R01EY011600 and P30EY014800, and in part by an unrestricted departmental grant from Research to Prevent Blindness. The FLIO instrument was provided to the Moran Eye Center by Heidelberg Engineering for no cost. The authors alone are responsible for the content and writing of the paper.

Disclosure: **L. Sauer**, Novartis (C); **C.B. Komanski**, None; **A.S. Vitale**, None; **E.D. Hansen**, None; **P.S. Bernstein**, None

References

1. Klein R, Klein BE, Jensen SC, Meuer SM. The five-year incidence and progression of age-related maculopathy: the Beaver Dam Eye Study. *Ophthalmology*. 1997;104:7–21.
2. Friedman DS, O'Colmain BJ, Munoz B, et al. Prevalence of age-related macular degeneration in the United States. *Arch Ophthalmol*. 2004;122:564–572.
3. Klein R, Cruickshanks KJ, Nash SD, et al. The prevalence of age-related macular degeneration and associated risk factors. *Arch Ophthalmol*. 2010;128:750–758.
4. Munk MR, Ceklic L, Ebneter A, Huf W, Wolf S, Zinkernagel MS. Macular atrophy in patients with long-term anti-VEGF treatment for neovascular age-related macular degeneration. *Acta Ophthalmol*. 2016;94:e757–e764.
5. Bernstein PS, Li B, Vachali PP, et al. Lutein, zeaxanthin, and meso-zeaxanthin: the basic and clinical science underlying carotenoid-based nutritional interventions against ocular disease. *Prog Retin Eye Res*. 2016;50:34–66.
6. Gorusupudi A, Nelson K, Bernstein PS. The Age-Related Eye Disease 2 Study: micronutrients in the treatment of macular degeneration. *Adv Nutr*. 2017;8:40–53.
7. Meyers SM, Greene T, Gutman FA. A twin study of age-related macular degeneration. *Am J Ophthalmol*. 1995;120:757–766.
8. Seddon JM, Ajani UA, Mitchell BD. Familial aggregation of age-related maculopathy. *Am J Ophthalmol*. 1997;123:199–206.
9. Hammond CJ, Webster AR, Snieder H, Bird AC, Gilbert CE, Spector TD. Genetic influence on early age-related maculopathy: a twin study. *Ophthalmology*. 2002;109:730–736.
10. Gehrs KM, Anderson DH, Johnson LV, Hageman GS. Age-related macular degeneration–emerging pathogenetic and therapeutic concepts. *Ann Med*. 2006;38:450–471.
11. Hageman GS, Mullins RF. Molecular composition of drusen as related to substructural phenotype. *Mol Vis*. 1999;5:28.
12. Hageman GS, Luthert PJ, Victor Chong NH, Johnson LV, Anderson DH, Mullins RF. An integrated hypothesis that considers drusen as biomarkers of immune-mediated processes at the RPE-Bruch's membrane interface in aging and age-related macular degeneration. *Prog Retin Eye Res*. 2001;20:705–732.
13. Anderson DH, Mullins RF, Hageman GS, Johnson LV. A role for local inflammation in the formation of drusen in the aging eye. *Am J Ophthalmol*. 2002;134:411–431.
14. Anderson DH, Radeke MJ, Gallo NB, et al. The pivotal role of the complement system in aging and age-related macular degeneration: hypothesis re-visited. *Prog Retin Eye Res*. 2010;29:95–112.
15. Pepple K, Mruthyunjaya P. Retinal pigment epithelial detachments in age-related macular degeneration: classification and therapeutic options. *Semin Ophthalmol*. 2011;26:198–208.
16. Schweitzer D, Hammer M, Schweitzer F, et al. In vivo measurement of time-resolved autofluorescence at the human fundus. *Biomed Opt*. 2004;9:1214–1222.
17. Schweitzer D, Schenke S, Hammer M, et al. Towards metabolic mapping of the human retina. *Microsc Res Tech*. 2007;70:410–419.
18. Schweitzer D. Metabolic mapping. In: Holz F, Spaide R, eds. *Medical Retina*. Berlin: Springer; 2010:107–123.
19. Klemm M, Dietzel A, Haueisen J, Nagel E, Hammer M, Schweitzer D. Repeatability of autofluorescence lifetime

imaging at the human fundus in healthy volunteers. *Curr Eye Res*. 2013;38:793–801.

20. Dysli C, Quellec G, Abegg M, et al. Quantitative analysis of fluorescence lifetime measurements of the macula using the fluorescence lifetime imaging ophthalmoscope in healthy subjects. *Invest Ophthalmol Vis Sci*. 2014;55:2106–2113.
21. Sauer L, Schweitzer D, Ramm L, Augsten R, Hammer M, Peters S. Impact of macular pigment on fundus autofluorescence lifetimes. *Invest Ophthalmol Vis Sci*. 2015;56:4668–4679.
22. Schweitzer D, Gaillard ER, Dillon J, et al. Time-resolved autofluorescence imaging of human donor retina tissue from donors with significant extramacular drusen. *Invest Ophthalmol Vis Sci*. 2012;53:3376–3386.
23. Sauer L, Gensure RH, Andersen KM, et al. Patterns of fundus autofluorescence lifetimes in eyes of individuals with nonexudative age-related macular degeneration. *Invest Ophthalmol Vis Sci*. 2018;59:AMD65–AMD77.
24. Dysli C, Fink R, Wolf S, Zinkernagel MS. Fluorescence lifetimes of drusen in age-related macular degeneration. *Invest Ophthalmol Vis Sci*. 2017;58:4856–4862.
25. Lakowicz JR, Szmacinski H, Nowaczyk K, Johnson ML. Fluorescence lifetime imaging of free and protein-bound NADH. *Proc Natl Acad Sci U S A*. 1992;89:1271–1275.
26. Lakowicz JR. *Principles of Fluorescence Spectroscopy*: Berlin: Springer; 2007.
27. Schweitzer D, Deutsch L, Klemm M, et al. Fluorescence lifetime imaging ophthalmoscopy in type 2 diabetic patients who have no signs of diabetic retinopathy. *J Biomed Opt*. 2015;20:61106.
28. Dysli C, Wolf S, Zinkernagel MS. Fluorescence lifetime imaging in retinal artery occlusion. *Invest Ophthalmol Vis Sci*. 2015;56:3329–3336.
29. Dysli C, Wolf S, Tran HV, Zinkernagel MS. Autofluorescence lifetimes in patients with choroideremia identify photoreceptors in areas with retinal pigment epithelium atrophy. *Invest Ophthalmol Vis Sci*. 2016;57:6714–6721.
30. Dysli C, Wolf S, Hatz K, Zinkernagel MS. Fluorescence lifetime imaging in stargardt disease: potential marker for disease progression. *Invest Ophthalmol Vis Sci*. 2016;57:832–841.
31. Dysli C, Wolf S, Zinkernagel MS. Autofluorescence lifetimes in geographic atrophy in patients with age-related macular degeneration. *Invest Ophthalmol Vis Sci*. 2016;57:2479–2487.
32. Dysli C, Berger L, Wolf S, Zinkernagel MS. Fundus autofluorescence lifetimes and central serous chorioretinopathy. *Retina*. 2017;37:2151–2161.
33. Dysli C, Wolf S, Berezin MY, Sauer L, Hammer M, Zinkernagel MS. Fluorescence lifetime imaging ophthalmoscopy. *Prog Retin Eye Res*. 2017;60:120–143.
34. Sauer L, Peters S, Schmidt J, et al. Monitoring macular pigment changes in macular holes using fluorescence lifetime imaging ophthalmoscopy. *Acta Ophthalmol*. 2017;95:481–492.
35. Schmidt J, Peters S, Sauer L, et al. Fundus autofluorescence lifetimes are increased in non-proliferative diabetic retinopathy. *Acta Ophthalmol*. 2017;95:33–40.
36. Dysli C, Schurch K, Pascal E, Wolf S, Zinkernagel MS. Fundus autofluorescence lifetime patterns in retinitis pigmentosa. *Invest Ophthalmol Vis Sci*. 2018;59:1769–1778.
37. Sauer L, Andersen KM, Dysli C, Zinkernagel MS, Bernstein PS, Hammer M. Review of clinical approaches in fluorescence lifetime imaging ophthalmoscopy. *J Biomed Opt*. 2018;23:1–20.
38. Andersen KM, Sauer L, Gensure RH, Hammer M, Bernstein PS. Characterization of retinitis pigmentosa using fluorescence lifetime imaging ophthalmoscopy (FLIO). *Trans Vis Sci Tech*. 2018;7(3):20.
39. Sauer L, Gensure RH, Hammer M, Bernstein PS. Fluorescence lifetime imaging ophthalmoscopy: a novel way to assess macular telangiectasia type 2. *Ophthalmol Retina*. 2018;2:587–598.
40. Sauer L, Klemm M, Peters S, et al. Monitoring foveal sparing in geographic atrophy with fluorescence lifetime imaging ophthalmoscopy - a novel approach. *Acta Ophthalmol*. 2018;96:257–266.
41. Becker W. *The bh TCSPC Handbook*. 6th ed. Berlin: Becker & Hickl GmbH; 2014.
42. Klemm M, Schweitzer D, Peters S, Sauer L, Hammer M, Haueisen J. FLIMX: A software package to determine and analyze the fluorescence lifetime in time-resolved fluorescence data from the human eye. *PLoS One*. 2015;10:e0131640.
43. Sauer L, Andersen KM, Li B, Gensure RH, Hammer M, Bernstein PS. Fluorescence lifetime imaging ophthalmoscopy (FLIO) of macular pigment. *Invest Ophthalmol Vis Sci*. 2018;59:3094–3103.
44. Khan KN, Mahroo OA, Khan RS, et al. Differentiating drusen: Drusen and drusen-like appearances associated with ageing, age-related macular degeneration, inherited eye disease and other pathological processes. *Prog Retin Eye Res*. 2016;53:70–106.
45. Schweitzer D, Kolb A, Hammer M, Anders R. Time-correlated measurement of autofluorescence. A method to detect metabolic changes in the fundus [in German]. *Ophthalmologe*. 2002;99:774–779.
46. Schweitzer D, Quick S, Schenke S, et al. Comparison of parameters of time-resolved autofluorescence between healthy subjects and patients suffering from early AMD [in German]. *Ophthalmologe*. 2009;106:714–722.
47. Schweitzer D. Autofluorescence diagnostics of ophthalmic diseases. In: Ghukasyan VV, Heikal AA, ed. *Natural Biomarkers for Cellular Metabolism-Biology, Techniques, and Applications*. Milton Park: Taylor & Francis Group; 2014:317–344.
48. Peters S, Hammer M, Schweitzer D. Two-photon excited fluorescence microscopy application for ex vivo investigation of ocular fundus samples. *Proc SPIE Int Soc Opt Eng*. 2011;8086:808605.
49. Hammer M, Sauer L, Klemm M, Peters S, Schultz R, Haueisen J. Fundus autofluorescence beyond lipofuscin: lesson learned from ex vivo fluorescence lifetime imaging in porcine eyes. *Biomed Opt Express*. 2018;9:3078–3091.
50. Guo K, Achilefu S, Berezin MY. Dating bloodstains with fluorescence lifetime measurements. *Chemistry*. 2012;18:1303–1305.
51. Schweitzer D, Hammer M, Schweitzer F. Limits of the confocal laser-scanning technique in measurements of time-resolved autofluorescence of the ocular fundus [in German]. *Biomed Tech (Berl)*. 2005;50:263–267.
52. Schweitzer D, Quick S, Klemm M, Hammer M, Jentsch S, Dawczynski J. Time-resolved autofluorescence in retinal vascular occlusions [in German]. *Ophthalmologe*. 2010;107:1145–1152.

Investigative Ophthalmology & Visual Science